Journal of Applied Mechanics and Technical Physics, Vol. 40, No. 4, 1999

NUMERICAL SIMULATION OF WAVE FLOWS CAUSED BY A SHORESIDE LANDSLIDE

V. V. Ostapenko

UDC 519.63

A mathematical model is developed for formation and propagation of discontinuous waves caused by sliding of a shoreside landslide into water. The model is based on the equations of a two-layer "shallow liquid" with specially introduced "dry friction" in the low layer, which allows one to describe the joint motion of the landslide and water. An explicit difference scheme approximating these equations is constructed, and it is used to develop a numerical algorithm for simulating the motion of the free boundaries of both the landslide and water (in particular, the propagation of a water wave along a dry channel, incidence of the wave on the lakeside, and flow over obstacles).

1. Mathematical Model for the Joint Motion of a Landslide and Water. In the present paper, the sliding of a lakeside landslide and the simultaneous wave motion of water caused by it are studied on the basis of the mathematical model of the first approximation of two-layer "shallow-water" theory [1, 2]. Use of this mathematical model to describe the process considered involves the following assumptions.

1. The motion of a landslide can be treated as motion of an incompressible liquid in which the special features of landslide motion compared to the liquid are taken into account in so-called "dry friction." This approach to studying landslides is proposed by Grigoryan et al. [3].

2. The depths of the moving landslide and water remain an order of magnitude smaller than the linear dimensions of the landslide and lake, respectively. Hence, the motion of each of them can be described using one of the models of shallow-water theory [2, 4, 5]. In the present work, we employ the first approximation of this theory, which implies the assumption of hydrostatic pressure (its linear dependence on the depth) and leads, in the one-layer case, to the St. Venant equations [4].

3. When the landslide enters water and moves under it, the landslide and water masses are poorly mixed. This allows one to describe their joint motion using the first approximation of two-layer "shallow-liquid" theory [1, 2].

Under the above assumptions, the standard (spatially two-dimensional) differential equations for joint motion of the landslide and water in Cartesian coordinates (t, x, y) have the form

$$\frac{\partial h}{\partial t} + \operatorname{div} \boldsymbol{q} = 0, \tag{1.1}$$

$$\frac{\partial q}{\partial t} + \operatorname{div}(\boldsymbol{v} \otimes \boldsymbol{q}) + gh\nabla z = \boldsymbol{f}, \tag{1.2}$$

$$\frac{\partial H}{\partial t} + \operatorname{div} \boldsymbol{Q} = 0, \tag{1.3}$$

$$\frac{\partial \boldsymbol{Q}}{\partial t} + \operatorname{div}(\boldsymbol{V} \otimes \boldsymbol{Q}) + gh\nabla(Z + \lambda h) = \boldsymbol{F}_{\text{liq}} - \lambda \boldsymbol{f} + \boldsymbol{F}_{\text{dry}}, \tag{1.4}$$

Lavrent'ev Institute of Hydrodynamics, Siberian Division, Russian Academy of Sciences, Novosibirsk 630090. Translated from Prikladnaya Mekhanika i Tekhnicheskaya Fizika, Vol. 40, No. 4, pp. 109–117, July–August, 1999. Original article submitted July 31, 1997.

0021-8944/99/4004-0647 $22.00

where h is the water depth, $z = Z+h$ is the water level, $\boldsymbol{q} = (q_1, q_2)$ is the water flow rate, $\boldsymbol{v} = (v_1, v_2) = \boldsymbol{q}/h$ is the water velocity averaged along the vertical, and H, $Z = z_{\text{bot}} + H$, $\boldsymbol{Q} = (Q_1, Q_2)$, and $\boldsymbol{V} = (V_1, V_2) = \boldsymbol{Q}/H$ are the same for the landslide, z_{bot} is the mark of the lake bottom or the coast level, g is the acceleration due to gravity, $\lambda = r/R < 1$ is the ratio of the water density r to the density of the landslide R, $\boldsymbol{f}$ is the force of friction between the water and the landslide, and $\boldsymbol{F}_{\text{liq}}$ and $\boldsymbol{F}_{\text{dry}}$ are the forces of "liquid" and "dry" frictions of the landslide on the bottom.

Because system (1.1)–(1.4) is spatially two-dimensional, all the functions included in it depend on the following three independent variables: the time t and the two spatial coordinates x and y. Hence, the differential operators div, ∇, and **div** included in the left sides of Eqs. (1.1)–(1.4) on each scalar function $z(t,x,y)$ and vector functions $\boldsymbol{q}(t,x,y) = (q_1, q_2)$ and $\boldsymbol{v}(t,x,y) = (v_1, v_2)$ act according to the formulas

$$\operatorname{div} \boldsymbol{q} = \frac{\partial q_1}{\partial x} + \frac{\partial q_2}{\partial y}, \qquad \nabla z = \left(\frac{\partial z}{\partial x}, \frac{\partial z}{\partial y}\right),$$

$$\mathbf{div}(\boldsymbol{v} \otimes \boldsymbol{q}) = \left(\frac{\partial}{\partial x}(v_1 q_1) + \frac{\partial}{\partial y}(v_2 q_1),\ \frac{\partial}{\partial x}(v_1 q_2) + \frac{\partial}{\partial y}(v_2 q_2)\right).$$

The vector of friction between the water and the landslide $\boldsymbol{f}$ and the vector of "fluid friction" of the landslide on the bottom $\boldsymbol{F}_{\text{liq}}$ are calculated as follows:

$$\boldsymbol{f} = -kg(\boldsymbol{v} - \boldsymbol{V})|\boldsymbol{v} - \boldsymbol{V}|, \qquad \boldsymbol{F}_{\text{liq}} = -KgV|V|; \tag{1.5}$$

$$k = n^2/h^{1/3}, \quad K = N^2/H^{1/3}. \tag{1.6}$$

Here k and K are the friction factors determined from the Manning formulas [4], n is the roughness factor for the landslide, and N is the effective factor of roughness between the landslide and the bottom.

The vector $\boldsymbol{F}_{\text{dry}}$ of "dry friction" of the landslide on the bottom is calculated from the formula

$$\boldsymbol{F}_{\text{dry}} = \begin{cases} -\gamma\theta PV/|V|, & V \neq 0, \\ \theta P\Phi/|\Phi|, & V = 0, \quad |\Phi| > \theta P, \\ \Phi, & V = 0, \quad |\Phi| < \theta P, \end{cases} \tag{1.7}$$

where

$$P = (rgh + RgH)/R = g(H + \lambda h). \tag{1.8}$$

Here P is the specific pressure of the landslide on the bottom, $\Phi = gH\nabla(Z + \lambda h)$ is the force acting on unit mass of the landslide in the horizontal direction,

$$\gamma = 1/(1 + a|V|^2), \qquad a = \text{const} > 0; \tag{1.9}$$

$\theta = \tan\beta$ is the factor of "dry friction" of the landslide on the bottom, and β is the so-called [3] angle of internal friction in the landslide (the maximum angle between the horizontal plane and the plane tangent to the surface of the landslide at which the originally immovable landslide remains still immovable). The introduction of the empirical factor (1.9) into (1.7) is due to the assumption that with increase in the speed of propagation of the landslide, the influence of "dry friction" rapidly decreases, and at rather high speeds, the motion of the landslide becomes completely similar to the motion of an incompressible liquid.

2. Simulation of Discontinuous Solutions. Since system (1.1)–(1.4) admits discontinuous solutions with discontinuous waves, on these waves we must specify relations that connect the flow parameters on both sides of the wavefront. The classical method of deriving a complete system of such relations (Hugoniot conditions) assumes the presence of a complete set of basic conservation laws [6, 7] that admits a closing conservation law which is used to select stable discontinuous solutions [8]. In gas dynamics, the basic system is the system of laws of conservation of mass, momentum, and total energy and the closing law is the law of conservation of entropy [6, 7]. In calculations of discontinuous waves using the Saint-Venant equations of the first approximation of "shallow water" theory, the system of laws of conservation of mass and total momentum is adopted [4, 7] as the basic system and the conservation law of total energy is considered the closing equation.

By analogy with the one-layer case, as the basic conservation laws for system (1.1)–(1.4), we take the laws of conservation of mass in layers (1.1) and (1.3) and the law of conservation of the total momentum

$$\frac{\partial}{\partial t}(\boldsymbol{Q}+\lambda\boldsymbol{q})+\operatorname{div}(\boldsymbol{V}\otimes\boldsymbol{Q}+\lambda\boldsymbol{v}\otimes\boldsymbol{q})+\frac{g}{2}\nabla(H^2+\lambda h^2+2\lambda hH)=\boldsymbol{F}_{\text{liq}}+\boldsymbol{F}_{\text{dry}}-g(H+\lambda h)\nabla z_0, \tag{2.1}$$

and as the closing equation, we use the law of conservation of the total energy

$$\frac{\partial e}{\partial t}+\operatorname{div}E=G, \tag{2.2}$$

where

$$e=\boldsymbol{Q}\cdot\boldsymbol{V}+\lambda\boldsymbol{q}\cdot\boldsymbol{v}+g(H^2+\lambda h^2+2h\lambda H),$$

$$E=[\boldsymbol{Q}\cdot\boldsymbol{V}+2gH(H+\lambda h)]\boldsymbol{V}+\lambda[\boldsymbol{q}\cdot\boldsymbol{v}+2gh(h+H)]\boldsymbol{v},$$

$$G=2[(\boldsymbol{F}_{\text{liq}}+\boldsymbol{F}_{\text{dry}})\cdot\boldsymbol{V}+\lambda\boldsymbol{f}\cdot(\boldsymbol{V}-\boldsymbol{v})-g(\boldsymbol{Q}+\boldsymbol{q})\cdot\nabla z_0]$$

[the right sides of Eqs. (2.1) and (2.2) contain quantities that remain continuous on discontinuity surfaces and, hence, do not influence the Hugoniot conditions]. However, the system of basic conservation laws (1.1), (1.3), (2.1) is incomplete since it lacks one vector or two scalar conservation laws. Therefore, we define the stable discontinuous solutions of system (1.1)–(1.4) as the limiting (in the limit $\mu\to 0$) solutions of the system obtained from (1.1)–(1.4) by supplementing the right sides of the momentum equations for the layers (1.2), and (1.4) with artificial viscosities

$$\boldsymbol{w}=\mu[\operatorname{div}(dry\nabla)]\boldsymbol{v},\quad \boldsymbol{W}=\mu[\operatorname{div}(dry\nabla)]\boldsymbol{V}, \tag{2.3}$$

where *dry* and *dry* are the positive-definite matrices of these viscosities [the viscosity $\boldsymbol{w}$ is added to Eq. (1.2) and the viscosity $\boldsymbol{W}$ to (1.4)].

The obtained limiting discontinuous solutions on discontinuity lines obey the laws of conservation of mass in the layers, the law of conservation of total momentum, and, in the weak sense, [8] the energy inequality

$$\frac{\partial e}{\partial t}+\operatorname{div}E<0, \tag{2.4}$$

which ensures their stability. Thus, because of the incompleteness of the basic conservation laws, the relation on discontinuity lines depends, generally speaking, on the particular form of the artificial viscosities *dry* and *dry* included in (2.3). However, as test calculations showed, this dependence is rather weak, and, hence, the matrices of the viscosities *dry* and *dry* in the difference scheme given below were chosen from purely computational considerations of minimum spread of the front of a discontinuous wave with simultaneous maintenance of its monotonic profile. These requirements are best satisfied by the coefficient matrices

$$c=\begin{pmatrix}|q_1| & |q_1|/2\\ |q_2|/2 & |q_2|\end{pmatrix},\qquad C=\begin{pmatrix}|Q_1| & |Q_1|/2\\ |Q_2|/2 & |Q_2|\end{pmatrix}, \tag{2.5}$$

which were used in numerical calculations.

3. Specification of the Initial Region of Solution and Initial and Boundary Conditions. We solve system (1.1)–(1.4) in the basic rectangular region

$$\Pi=\{0\leqslant x\leqslant X,\ 0\leqslant y\leqslant Y\}, \tag{3.1}$$

in which we specify the marks of the lake bottom or the coast level $Z_{\text{bot}}(x,y)$ and two (generally, multiply connected) subregions Ω_{w}, $\Omega_{\text{land}}\subseteq\Pi$, the first of which contains water at the initial time and in the second there is the landslide. In view of this, we specify the initial water level $z_0(x,y)$ in the region Ω_{w} and the initial level of the landslide $Z_0(x,y)$ in the region Ω_{land}. The initial depths are calculated from the formulas

$$H_0(x,y)=Z_0(x,y)-z_{\text{bot}}(x,y)\quad\forall(x,y)\in\Omega_{\text{land}},$$

$$h_0(x,y)=\begin{cases}z_0(x,y)-z_{\text{bot}}(x,y) & \forall(x,y)\in\Omega_{\text{w}}\setminus\Omega_{\text{land}},\\ z_0(x,y)-Z_0(x,y) & \forall(x,y)\in\Omega_{\text{w}}\cap\Omega_{\text{land}}.\end{cases}$$

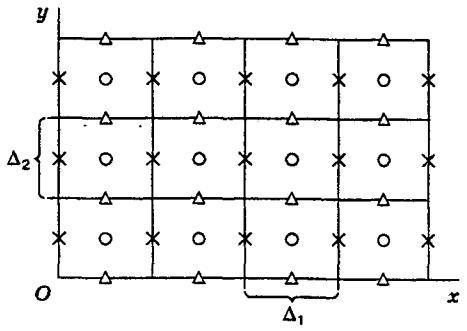

Fig. 1

The initial water velocity is considered zero, i.e., $\boldsymbol{v}_0 = 0$, and that of the landslide is constant, i.e., $\boldsymbol{V}_0 = \text{const}$. On the segments of the boundaries of the internal regions Ω_{w} and Ω_{land} that are not intersected with the boundary of the basic region (3.1), nonpenetration conditions are imposed:

$$\boldsymbol{v} \cdot \boldsymbol{n}_{\text{w}} = 0, \quad \boldsymbol{V} \cdot \boldsymbol{n}_{\text{land}} = 0. \tag{3.2}$$

Here $\boldsymbol{n}_{\text{w}}$ and $\boldsymbol{n}_{\text{land}}$ are unit normal vectors to the boundaries $\partial\Omega_{\text{w}}$ and $\partial\Omega_{\text{land}}$. On segments of these boundaries that lie on the boundary $\partial\Pi$ of the basic region (3.1), we impose the nonpenetration condition (3.2) or (assuming that the flow from the region is subcritical and locally one-dimensional) specify the value of the issuing invariant brought on the boundary $\partial\Pi$ along the characteristic that comes from region Π.

4. Simulation of the Calculation Region. System (1.1)–(1.4) is solved by a finite-difference method on a fixed uniform rectangular grid. The basic calculation region is a rectangle (3.1) divided into a certain number of identical rectangular cells (Fig. 1) with sides Δ_1 and Δ_2 along the x and y axes, respectively. Let us have $n_1 = X/\Delta_1$ cells on the x axis and cells $n_2 = Y/\Delta_2$ on the y axis (in Fig. 1, $n_1 = 4$ and $n_2 = 3$). The grid values of the scalar functions included in system (1.1)–(1.4) are specified at the centers of these cells, i.e., at points with the coordinates

$$\{((i+0.5)\Delta_1, (j+0.5)\Delta_2); \quad 0 \leqslant i \leqslant n_1 - 1, \quad 0 \leqslant j \leqslant n_2 - 1\} \tag{4.1}$$

(circles in Fig. 1). The values of the vector functions $\boldsymbol{f} = (f_1, f_2)$ are specified on the boundaries of these cells: the first components f_1 are defined in the middles of the vertical sides of the cells (crosses in Fig. 1), i.e., at points with the coordinates

$$\{(i\Delta_1, (j+0.5)\Delta_2); \quad 0 \leqslant i \leqslant n_1, \quad 0 \leqslant j \leqslant n_2 - 1\}, \tag{4.2}$$

and the second components f_2 are specified in the middles of the horizontal sides of the cells (triangles in Fig. 1), i.e., at points with the coordinates

$$\{((i+0.5)\Delta_1, j\Delta_2); \quad 0 \leqslant i \leqslant n_1 - 1, \quad 0 \leqslant j \leqslant n_2\}. \tag{4.3}$$

The motion of the free boundaries of the liquid and landslide within the basic fixed calculation region (3.1) is simulated using the method of "fictitious cells" [9]. In this case, for the water and landslide, we introduce auxiliary arrays k_{ij}^n and K_{ij}^n, which take only two different values ± 1 at the center of each calculation cell:

$$\alpha_{ij} = \{(x, y): \ i\Delta_1 \leqslant x \leqslant (i+1)\Delta_1, \ j\Delta_2 \leqslant y \leqslant (j+1)\Delta_2\} \subset \Pi.$$

Using these arrays, in each nth time layer, we form internal calculation regions:

$$\Omega_{\text{w}}^n = \{\alpha_{ij} \subset \Pi : k_{ij}^n = 1\}, \quad \Omega_{\text{land}}^n = \{\alpha_{ij} \subset \Pi : K_{ij}^n = 1\}.$$

We describe the variation of these regions using as an example the region Ω_{w}^n, which contains water. For this, we introduce the small number $\varepsilon > 0$ and define

$$h_{ij}^0 = h(0, (i+0.5)\Delta_1, (j+0.5)\Delta_2) = \varepsilon \quad \forall k_{ij}^0 = -1 \qquad (\forall \alpha_{ij} \not\subset \Omega_{\text{w}}^0),$$

i.e., at the initial time, we artificially "pour an ε-layer of water" on the coast. If as a result of calculation, we obtain $h_{ij}^{n+1} \leqslant \varepsilon$ in a certain cell $\alpha_{ij} \subset \Omega_{\mathrm{w}}^n$, we assume that $h_{ij}^{n+1} = \varepsilon$ in this cell. If in each cell adjacent to the cell α_{ij} (i.e., having with it a common side), it turned out that $h^{n+1} = \varepsilon$ or $z^{n+1} \leqslant z_{ij}^{n+1}$, the cell α_{ij} becomes "non-working" (or "dummy") in the $(n+1)$th time layer, i.e., $\alpha_{ij} \not\subset \Omega_{\mathrm{w}}^{n+1}$ $(k_{ij}^{n+1} = -1)$. On the other hand, if in a certain cell adjacent to the "non-working" cell in the nth time layer $\alpha_{ij} \not\subset \Omega_{\mathrm{w}}^n$ $(k_{ij}^n = -1)$ we find that, simultaneously, $h^{n+1} > \varepsilon$ and $z^{n+1} > z_{ij}^{n+1}$, this cell α_{ij} becomes "working" in the $(n+1)$th time layer, i.e., $\alpha_{ij} \subset \Omega_{\mathrm{w}}^{n+1}$ $(k_{ij}^{n+1} = 1)$.

Variation in the internal calculation region Ω_{land}^n, which contains the landslide, occurs similarly.

5. Difference Scheme. As the difference scheme approximating system (1.1)–(1.4), we use an analog of the "cross" scheme, which is well known in gas dynamics [10]. The following notation, which is partially borrowed from [11], is used: $f = f_{ij}^n$, where the superscript n denotes the nth time layer and the pair of subscripts (i,j) denote the node (4.1) for scalar quantities, the node (4.2) for the first component, the node (4.3) for the second component of the vector quantities, and the node $\{(i\Delta_1, j\Delta_2);\quad 0 \leqslant i \leqslant n_1,\ 0 \leqslant j \leqslant n_2\}$ for the auxiliary quantities u and U, defined by the formulas

$$u = q_{1(y)}q_{2(x)}/h^*, \quad U = Q_{1(y)}Q_{2(x)}/H^*,$$

where $f_{(x)} = (f_{i,j}^n + f_{i-1,j}^n)/2$, $f_{(y)} = (f_{i,j}^n + f_{i,j-1}^n)/2$, and $f^* = (f_{i,j}^n + f_{i-1,j}^n + f_{i,j-1}^n + f_{i-1,j-1}^n)/4$.

For the finite-difference relations, we use the following notation: $f_t = (f_{i,j}^{n+1} - f_{i,j}^n)/\tau_n$, $f_{t-} = (f_{i,j}^b - f_{i,j}^n)/\tau_n$, $f_{t+} = (f_{i,j}^{n+1} - f_{i,j}^b)/\tau_n$, $f_x = (f_{i+1,j}^n - f_{i,j}^n)/\Delta_1$, $f_{\bar{x}} = (f_{i,j}^n - f_{i-1,j}^n)/\Delta_1$, $f_{2x} = (f_{i+1,j}^n - f_{i-1,j}^n)/(2\Delta_1)$, $f_y = (f_{i,j+1}^n - f_{i,j}^n)/\Delta_2$, $f_{\bar{y}} = (f_{i,j}^n - f_{i,j-1}^n)/\Delta_2$, and $f_{2y} = (f_{i,j+1}^n - f_{i,j-1}^n)/(2\Delta_2)$, where τ_n is the step of the scheme in the nth time layer and $f_{i,j}^b$ is an auxiliary value of the grid function $f_{i,j}^n$.

Calculations in each new $(n+1)$th time layer are performed in four steps.

In the first step, the depths $h_{i,j}^{n+1}$ and $H_{i,j}^{n+1}$ and the levels $z_{i,j}^{n+1}$ and $Z_{i,j}^{n+1}$ are calculated by the explicit scheme

$$h_t + q_{1x} + q_{2y} = 0, \quad H_t + Q_{1x} + Q_{2y} = 0, \quad Z^+ = x_{\mathrm{bot}} + H^+, \quad z^+ = Z^+ + h^+,$$

where $f^+ = f_{i,j}^{n+1}$. For the following three steps, we give difference equations only for the x components of the velocities and flow rates (the equations for the y components are written similarly). Therefore, the subscript 1 for the first components of the flow rates, velocities, and viscosities is dropped for brevity.

In the second step, the auxiliary values of the flow rates $q_{i,j}^b$ and $Q_{i,j}^b$ are calculated by the following semi-explicit scheme ignoring friction:

$$q_{t-} + (qv)_{2x} + u_y + gh_{(x)}^+ Z_{\bar{x}}^+ = w, \qquad Q_{t-} + (QV)_{2x} + U_y + gH_{(x)}^+ (Z^+ + \lambda h^+)_{\bar{x}} = W.$$

Here w and W are the linear artificial viscosities, which, with allowance for (2.3) and (2.5), are determined from the formulas

$$w = C_1\Delta_1\Big[(|q_{(x)}|v_{\bar{x}})_x + \Big(\frac{1}{2}|q_{(y)}|v_{\bar{y}}\Big)_y\Big], \qquad W = C_2\Delta_1\Big[(|Q_{(x)}|V_{\bar{x}})_x + \Big(\frac{1}{2}|Q_{(y)}|V_{\bar{y}}\Big)_y\Big],$$

where C_1 and $C_2 = \mathrm{const}$.

In the third step, the final values of the flow rates $q_{i,j}^{n+1}$ and $Q_{i,j}^{n+1}$ are calculated by the implicit scheme taking into account friction:

$$q_{t+} = f^+, \quad Q_{t+} = F_{\mathrm{liq}}^+ - \lambda f^+ + F_{\mathrm{dry}}^+, \tag{5.1}$$

where, according to (1.5)–(1.8),

$$f^+ = -kg(q^+/h_{(x)}^+ - Q^+/H_{(x)}^+)|\boldsymbol{v} - \boldsymbol{V}|, \qquad F_{\mathrm{liq}}^+ = -KgQ^+|\boldsymbol{V}|/H_{(x)}^+,$$
$$F_{\mathrm{dry}}^+ = \gamma\theta g(H^+ + \lambda h^+)Q^+/(H_{(x)}^+|V|), \quad \boldsymbol{V} \neq 0. \tag{5.2}$$

Equations (5.1) subject to (5.2) at each node i,j represent a system of two equations for two unknowns q^+ and Q^+. Solution of this system gives the flow rates in the $(n+1)$th time layer.

At the final fourth step, the velocities $v_{i,j}^{n+1}$ and $V_{i,j}^{n+1}$ are calculated from the formulas

$$v^+ = q^+/h^+_{(x)}, \quad V^+ = Q^+/H^+_{(x)}$$

and the new step in time is determined:

$$\tau_{n+1} = A\Delta/\max_{ij}\max(\sqrt{gh^+} + |v^+|, \sqrt{gH^+} + |V^+|). \tag{5.3}$$

Here $A = \text{const} < 1/2$ is the margin factor and $\Delta = \min(\Delta_1, \Delta_2)$.

The above difference scheme (5.3) taking into account the "implicit" friction (5.1) is a stable Courant's scheme in a linear approximation. It admits explicit implementation and approximates the laws of conservation of mass in layers (1.1) and (1.3) with a second order in space. In the absence of artificial viscosity ($\boldsymbol{w} = \boldsymbol{W} = 0$), it also approximates the laws of conservation of momentum (1.2) and (1.4) with a second order in space.

The scheme proposed here is almost conservative in the sense that it approximates in a conservative fashion [12] the laws of conservation of mass in layers (1.1) and (1.3), the law of conservation of the total momentum (2.1), and, with accuracy up to $o(\Delta)$, it satisfies the difference analog of the energy inequality (2.4). By virtue of this, the limiting discontinuous shock-wave solutions obey the laws of conservation of mass in the layers and total momentum and are stable in the sense of satisfaction of the energy inequality (2.4).

It should be noted that the scheme developed here is one of the most effective simple first-order-approximation schemes for through calculations of discontinuous solutions of system (1.1)–(1.4). With optimal choice of the artificial viscosities C_1 and C_2, it spreads discontinuities onto 3 or 4 spatial intervals without marked numerical oscillations. The main disadvantage of this scheme (like any other first-order-approximation scheme) is that the width of the spread of the front of a discontinuous wave depends of on its intensity (this width decreases in proportion to the increase in wave intensity). Therefore, for each particular calculation, there is particular optimum viscosity, which should be chosen specially.

6. Test Calculations. This section describes test calculations of spatially one-dimensional flows by the difference scheme proposed above. As a first example (Fig. 2), we consider one-layer liquid flow, and as second and third examples (Fig. 3 and 4), two-layer liquid flow. In the first two examples, we examine the flow over a horizontal bottom ignoring friction. In all the calculations, it was assumed that $\Delta = 0.1$, $A = 0.4$, and $g = 10$.

Figure 2 gives, for a time $T = 0.5$, results of calculation of the classical test problem of the failure of a dam [4], i.e., the problem of decay of an initial discontinuity of depth:

$$h(0,x) = \begin{cases} 3{,}4122 & \text{for } 0 \leqslant x \leqslant 4, \\ 1 & \text{for } 4 < x \leqslant 8 \end{cases} \tag{6.1}$$

in quiescent water. The exact solution of this problem gives a discontinuous wave propagating at constant speed and a falling wave. This exact solution is shown in Fig. 2 by a solid curve and the corresponding difference solution is shown by circles. The dashed curve shows the initial water surface defined by function (6.1).

Figure 3 gives the results of calculation of the problem of decay of an initial discontinuity of the interface of a quiescent liquid at a time $T = 0.5$:

$$z(0,x) = 3, \quad q(0,x) = Q(0,x) = 0, \qquad Z(0,x) = \begin{cases} 2.5 & \text{for } 0 \leqslant x \leqslant 4, \\ 0.5 & \text{for } 4 < x \leqslant 8. \end{cases} \tag{6.2}$$

Large circles show the calculated interface between the layers and small circles show the free surface of the upper layer. In the calculations, we set $\lambda = 0.3$, $C_1 = 1$, and $C_2 = 0.3$. The solid curve shows the initial interface between the layers (6.2) of the two-layer liquid, and the dashed curve shows the unperturbed surface of the upper layer.

Figure 3 show the results of numerical solution of this problem. It is evident that in the upper layer two waves propagating in different directions form: a rising wave, which propagates to the right, and a falling wave, which propagates to the left. These waves have almost equal amplitudes and velocities.

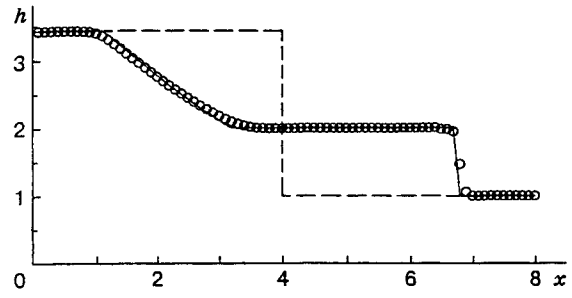

Fig. 2

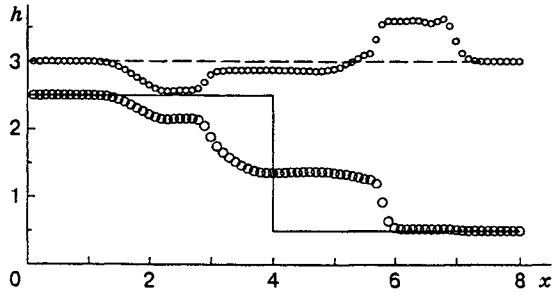

Fig. 3

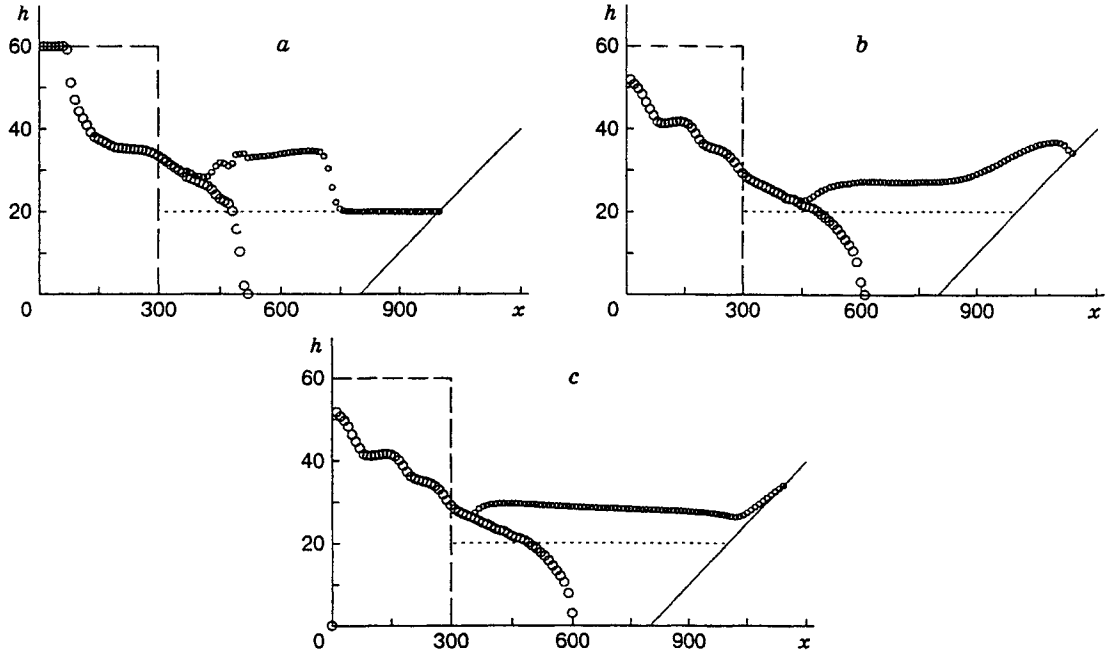

Fig. 4

Figure 4 shows, for three successive times, results of one-dimensional numerical modeling of the sliding of a shoreside landslide into water, formation and propagation of the discontinuous water wave that arises in this case, and incidence of the wave on the opposite sloping shore. The solid curve shows the bottom, the dashed curve shows the initial position of the landslide, and the dotted curve the initial position of the free water surface. The large circles show the calculated surface of the landslide, and the small circles the calculated free water surface. The scale in Fig. 4 is given in meters, and it is different on different axes: on the Ox axis, it is approximately 13 times smaller than on the Oh axis. In this calculation, it was assumed that $\lambda = 0.3$, $n = N = 0.25$, $a = 0.2$, $\theta = 0.3$, $C_1 = 7.5$, and $C_2 = 15$.

The initial stage of entry of the landslide in water and formation of an discontinuous water wave at $T = 20$ sec is shown Fig. 4a, and the moment of maximum incidence of the water wave on the opposite sloping lakeside at $T = 60$ sec is shown in Fig. 4b. Figure 4c shows the moment $T = 100$ sec when the water wave reflected from the sloping lakeside in the right part of the figure begins to flow on the surface of the landslide which has already come down and is immovable at this time. In this case, allowance for "dry friction" (1.7) ($\theta \neq 0$) leads to the landslide surface being not horizontal at the moment of establishment.

In conclusion we note that the numerical algorithm described in the present paper was used in [13, 14] for calculations of the formation, propagation, and overflow through the Usoi slide rock of the discontinuous

water wave produced by the sliding of a shoreside landslide into Sarez lake (Tadjikistan).

This work was supported by the Russian Foundation for Fundamental Research (Grant Nos. 96-01-01546 and 96-01-01547).

REFERENCES

1. L. V. Ovsyannikov, "Models of two-layer 'shallow water'," *Prikl. Mekh. Tekh. Fiz.*, No. 2, 3–14 (1979).
2. L. V. Ovsyannikov, N. I. Makarenko, V. I. Nalimov, et al., *Nonlinear Problems of the Theory of Surface and Internal Waves* [in Russian], Nauka, Novosibirsk (1985).
3. S. S. Grigoryan, N. N. Nilov, A. V. Ostroumov, V. S. Fedorenko, "Mathematical modeling of mountain landslides and landslides of large volumes," *Inzh. Geologiya*, No. 6, 61–72 (1983).
4. J. J. Stoker, *Water Waves. Mathematical Theory and Applications*, Interscience Publishers, New York (1957).
5. A. A. Atavin and S. M. Shugrin, "On the differential 'shallow-water' equations," in: *Dynamics of Continuous Media* (collected scientific papers) [in Russian], Novosibirsk, **70** (1985), pp. 25–53.
6. B. L. Rozhdestvenskii and N. N. Yanenko. *Systems of Quasi-Linear Equations and Their Applications to Gas Dynamics* [in Russian], Nauka, Moscow (1978).
7. A. F. Voevodin and S. M. Shugrin, *Methods of Solving One-Dimensional Evolutionary Systems* [in Russian], Nauka, Novosibirsk (1993).
8. P. D. Lax, *Hyperbolic Systems of Conservation Laws and the Mathematical Theory of Shock Waves*, Soc. Industr. and Appl. Math., Philadelphia (1972).
9. O. M. Belotserkovskii and Yu. M. Davydov, *Coarse-Particle Method in Gas Dynamics. Computational Experiment* [in Russian], Nauka, Moscow (1982).
10. V. E. Troshchiev, "Divergence of the cross scheme for numerical solution of the equations of gas dynamics," in: *Numerical Methods of Continuum Mechanics* (collected scientific paper) [in Russian], Inst. of Theor. and Appl. Mech., Vol. 1, No. 5 (1970), pp. 79–91.
11. A. A. Samarskii and Yu. P. Popov, *Difference Methods of Solving Problems of Gas Dynamics* [in Russian], Nauka, Moscow (1980).
12. V. V. Ostapenko, "On equivalent definitions of the concept of conservatism for finite-difference schemes," *Zh. Vychisl. Mat. Mat. Fiz.*, 29, No. 8, 1114–1128 (1989).
13. V. V. Ostapenko, "Numerical modeling of wave flows in Sarez lake caused by catastrophic sliding of a lakeside landslide," *Vychisl. Tekhnol.* **3**, 116–125 (1994).
14. V. V. Ostapenko, "Numerical modeling of wave flows in Sarez lake caused by hazardous sliding of lakeside landslide," in: Proc. Int. Conf. AMCA-95 (Novosibirsk, June 20–24, 1995), NCC Publisher, Novosibirsk (1995), pp. 212–217.